

# Electron quantum interference in epitaxial antiferromagnetic NiO thin films

Cite as: AIP Advances 10, 045204 (2020); doi: 10.1063/1.5129772

Presented: 5 November 2019 • Submitted: 1 October 2019 •

Accepted: 16 March 2020 • Published Online: 3 April 2020



Jia Xu,<sup>1</sup> Feng Lou,<sup>1,2,3</sup> Mengwen Jia,<sup>1</sup>  Gong Chen,<sup>4</sup> Chao Zhou,<sup>1</sup> Qian Li,<sup>5</sup> Kai Liu,<sup>4,6</sup>  Andreas K. Schmid,<sup>7</sup> Hongjun Xiang,<sup>1,2,3</sup> and Yizheng Wu<sup>1,3,a)</sup> 

## AFFILIATIONS

<sup>1</sup>Department of Physics and State Key Laboratory of Surface Physics, Fudan University, Shanghai 200433, China

<sup>2</sup>Key Laboratory of Computational Physical Sciences (Ministry of Education), Fudan University, Shanghai 200433, China

<sup>3</sup>Collaborative Innovation Center of Advanced Microstructures, Nanjing 210093, China

<sup>4</sup>Department of Physics, University of California, Davis, California 95616, USA

<sup>5</sup>Department of Physics, University of California, Berkeley, California 94720, USA

<sup>6</sup>Physics Department, Georgetown University, Washington, DC 20057, USA

<sup>7</sup>Lawrence Berkeley National Laboratory, Berkeley, California 94720, USA

**Note:** This paper was presented at the 64th Annual Conference on Magnetism and Magnetic Materials.

**a)** Author to whom correspondence should be addressed: [wuyizheng@fudan.edu.cn](mailto:wuyizheng@fudan.edu.cn)

## ABSTRACT

The electron reflectivity from NiO thin films grown on Ag(001) has been systematically studied as a function of film thickness and electron energy. A strong electron quantum interference effect was observed from the NiO film, which is used to derive the unoccupied band dispersion above the Fermi surface along the  $\Gamma$ -X direction using the phase accumulation model. The experimental bands agree well with first-principles calculations. A weaker electron quantum interference effect was also observed from the CoO film.

© 2020 Author(s). All article content, except where otherwise noted, is licensed under a Creative Commons Attribution (CC BY) license (<http://creativecommons.org/licenses/by/4.0/>). <https://doi.org/10.1063/1.5129772>

## INTRODUCTION

Recently, antiferromagnetic (AFM) spintronics has drawn significant attention due to its potential for low power consumption information storage and ultrafast switching.<sup>1,2</sup> NiO, one of the most common AFM oxides, is a fascinating candidate for investigating many novel spin-dependent phenomena in AFM materials, such as spin Hall magnetoresistance,<sup>3–6</sup> enhanced spin current transmission,<sup>7–10</sup> THz magnons,<sup>11,12</sup> and the switching of AFM spins by the spin-orbit torque.<sup>13–15</sup> All those spin-dependent transport properties are closely correlated with the electronic structure of NiO, which motivates experimental studies of band dispersions, especially in the ultrathin film range.

Theoretically, the NiO band structure has been intensively studied. NiO is well known as an insulator,<sup>16</sup> but standard band theory predicted NiO to be metallic,<sup>16</sup> which triggered more detailed theoretical studies of the relatively large band gap of NiO.<sup>17–20</sup>

The band structure of NiO has been studied experimentally using x-ray photoelectron spectroscopy (XPS),<sup>21,22</sup> bremsstrahlung-isochromat spectroscopy (BIS)<sup>23</sup> and angle resolved photoemission spectroscopy (ARPES).<sup>24,25</sup> Here XPS and BIS detect the density of states, and ARPES reveals the band structure near or below the Fermi surface. However, band dispersion well above the Fermi surface has been rarely explored. On the other hand, unoccupied bands play critical roles in the optical excitation of electrons and spins, and have an important impact on the magneto-optic effect. Due to the promising applications of NiO films in AFM spintronics, it is important to study the unoccupied electronic structure of NiO ultrathin film, which can help to refine the knowledge of the unoccupied band structures above the Fermi energy.

Unoccupied band dispersions can be experimentally determined through the electron quantum interference effect in thin films, and has been done for a number of films including Fe,<sup>26</sup> Co,<sup>27,28</sup> Cu,<sup>29</sup> graphene,<sup>30</sup> and the insulator MgO.<sup>31</sup> In this work,

we report an experimental study on the electronic band structure of epitaxial NiO films grown on Ag(001). Using low energy electron microscopy, we measure the electron reflectivity as a function of NiO film thickness and electron energy. We find that the electron reflectivity from NiO films oscillates with both electron energy and film thickness. Our experimental data can be well described by the phase accumulation model,<sup>26–33</sup> which is used to derive the band dispersion along the  $\Gamma$ -X direction in the energy ranges of 4–7.5 eV and 14–22 eV above the Fermi surface. The energy bands of NiO are calculated using first principles, and results are in good agreement with our experimental data. Furthermore, measurements of electron reflectivity in a CoO/Ag(001) system, which has the same atomic structure as NiO, also show a weak quantum interference effect, suggesting the possibility to study the unoccupied band dispersion in CoO.

## EXPERIMENTS

Our experiments were performed in the spin-polarized low energy electron microscopy (SPLEEM) system at the National Center for Electron Microscopy at Lawrence Berkeley National Laboratory.<sup>34,35</sup> The SPLEEM measurements were performed on NiO/Ag(001) and CoO/Ag(001) thin films. The Ag(001) single crystal substrate was cleaned by cycles of Ar<sup>+</sup> ion sputtering at 800 eV and annealing at 450 °C. *In situ* Auger electron spectroscopy confirms that the Ag(001) surface is free of carbon and oxygen contaminants. Finally, the Ag(001) substrate is annealed at 450 °C in the SPLEEM chamber with a base pressure of  $2 \times 10^{-11}$  Torr. This procedure results in a surface morphology composed of large atomically flat terraces, which have the width of a few hundred angstroms. The high quality of Ag(001) substrate is confirmed by sharp spots in low energy electron diffraction (LEED) patterns, as shown in Fig. 1(a).

NiO(001) films were grown epitaxially on the Ag(001) substrate at room temperature by evaporating Ni at a rate of  $\sim 0.23$  monolayer (ML)/min with an oxygen pressure of  $1.0 \times 10^{-7}$  Torr. Figure 1(b) shows a LEED pattern from 15 ML NiO on Ag(001), which shows good epitaxial growth of the NiO film on Ag(001). The good quality of NiO film can also be confirmed from the LEEM image in Figure 1(c), with the absence of step bunches and large defects on the surface. The epitaxy relationship of NiO film on Ag(001) is NiO[100](001)//Ag[100](001), and the AFM spins in NiO film are along the in-plane  $\langle 110 \rangle$  directions.<sup>36</sup> Due to the lattice mismatch between Ag and NiO, there is compressive strain in the NiO film. In addition, CoO films were grown at room temperature, by evaporating Co at a rate of 0.84 ML/min under an oxygen pressure of  $8.0 \times 10^{-8}$  Torr. The film thickness is determined by monitoring the electron reflectivity oscillations associated with the atomic layer-by-layer growth. During the reflectivity measurements, it is experimentally challenging to maintain perfectly stable electron beam current, because the electron gun's efficiency degrades during the oxygen exposure. For this reason, the electron reflectivity measurements were performed step by step at every 0.25 ML NiO deposition. Prior to each electron reflectivity measurement, the oxygen is pumped from the SPLEEM chamber, the film is annealed to 300 °C for 2 minutes, and then cooled down to room temperature. In the SPLEEM system, the electron beam is directed to the sample surface at

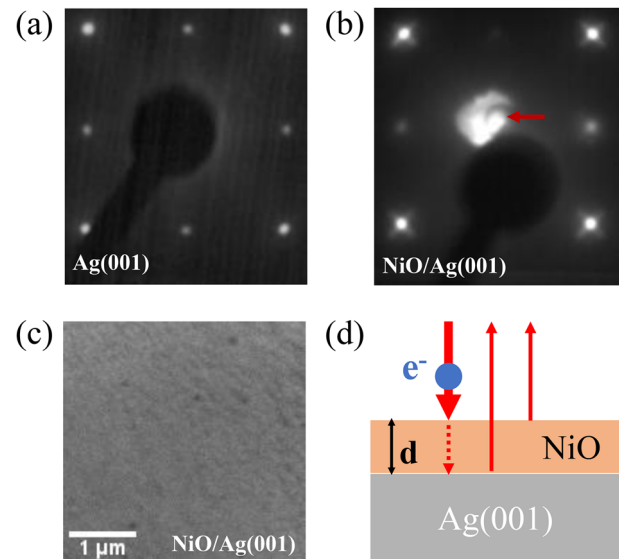


**FIG. 1.** (a) LEED pattern of Ag(001) at the electron energy  $E$  of 140 eV. (b) LEED pattern of 15 ML NiO film at  $E=151$  eV. The red arrow in (b) shows the electron specular beam. (c) LEEM image at  $E=4.1$  eV of NiO (15 ML) on Ag(001) substrate. (d) Schematic illustration of quantum interference effect of electrons in thin films with a thickness of  $d_{\text{NiO}}$ .

normal incidence, and the reflected specular beam is magnified by an electron-optical column to image the sample surface.<sup>26,31</sup> By varying the incident energy of electrons on the sample surface, we obtain the sample's reflectivity spectra as a function of the electron energy.<sup>26,31</sup> Since there is no net magnetic moment in the AFM NiO system, the reflectivity from the NiO surface is expected not to be sensitive to the spin polarization directions. In this paper, we only present the reflectivity results of unpolarized electrons by averaging the reflectivities of spin-up and spin-down electrons.

## RESULTS AND DISCUSSION

In the quantum interference measurements, the incident electron beam is normal to the thin film surface, and the electron reflectivity is measured as a function of the film thickness and electron energy. The quantum interference effect originates from the interference of electron reflection between the surface and the bottom interface of the film, as indicated in Fig. 1(d). Theoretically, the quantum interference effect has been well described by the so-called phase accumulation model,<sup>26–33</sup> which gives the quantization condition of:

$$2k(E)d_{\text{NiO}} + \varphi(E) = 2n\pi \quad (1)$$

where  $k(E)$  is the electron wave vector,  $n$  is an integer number,  $\varphi(E)$  is the total phase gain at the top/bottom surfaces of the NiO film. The phase  $\varphi$  changes with the electron energy, but is independent of the film thickness. For the electrons matching the quantization condition, the reflectivity should reach a maximum. As a result, the total reflectivity oscillates when either the energy or film thickness changes.

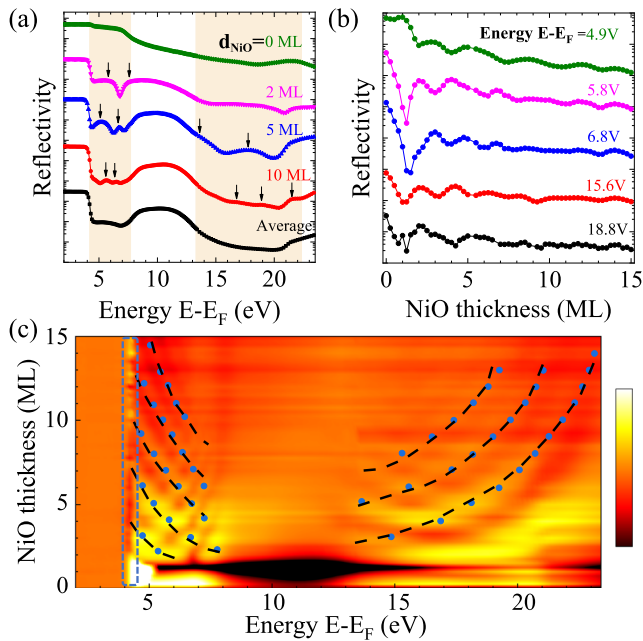


**FIG. 2.** (a) Electron reflectivity spectra of NiO films with different thickness as a function of electron energy. Black arrows indicate the oscillation peaks. Black curve shows the average spectrum of 3–15 ML NiO. (b) Electron reflectivity as a function of NiO thickness at several electron energies. (c) Normalized electron reflectivity as a function of NiO film thickness and the electron energy. The black dash lines are guide lines to show the peak evolutions of the electron reflectivity. The blue dots indicate peaks in the reflectivity. The blue rectangle indicates the area affected by the normalization process due to the change of work function as a function of NiO thickness.

Figure 2(a) shows typical reflectivity spectra of a NiO film grown on Ag(001) substrate with different NiO thicknesses. The electrons are fully reflected when the electron energy is below the work function, but the electron reflectivity drops very rapidly when the electron energy is above the sample's work function. Note that in this SPLEEM instrument, the electron energy approximately equals the sum of the sample bias voltage plus the 1.4 eV photon energy of the instrument's photoemission electron gun.<sup>29,31,34</sup> Significant oscillations of the reflectivity are observed in the electron energy range of 4–7.5 eV and 14–22 eV, as indicated by black arrows in

the orange regions in Fig. 2(a). For thicker NiO films, more oscillations with weaker amplitudes can be observed, until a NiO thickness of 15 ML. These reflectivity oscillations as a function of NiO thickness and electron energy result from the quantum interference effect,<sup>29,37,38</sup> where the electron reflectivity reaches maxima whenever the Fabry–Pérot interference between electron reflection at the NiO/vacuum surface and at the NiO/Ag interface satisfies the quantum interference condition of Eq. (1).

The strong reflectivity in the energy range of 8–13 eV for NiO films thicker than 2 ML is due to the band gap in the NiO film. Since there are no available electron states in the band gap, electrons within this energy range cannot penetrate into the NiO film, which leads to the high electron reflectivity within the band gap. Our results also indicate that the bulk energy gap of NiO film is well developed when the film is thicker than 2 ML.

We also analyzed the spectra measured at various fixed values of electron energy as a function of NiO thickness, as shown in Fig. 2(b). It is obvious that the reflectivity oscillates periodically with the film thickness, but the oscillation periods at different electron energies are different. Fig. 2(c) plots the electron reflectivity on a color scale, as a function of both film thickness (vertical axis) and electron energy (horizontal axis). To highlight the quantum interference, we normalized the spectra of NiO to the average spectrum of 3–15 ML.<sup>31</sup> The peaks in the normalized reflectivity are marked as blue dots in Fig. 2(b).

Electrons with the energy within the NiO energy bands can transmit into the NiO film and are partially reflected from the NiO/Ag interface, so that the electron reflected at NiO/Ag and NiO/vacuum interfaces can interfere with each other, leading to the reflectivity oscillations with both electron energy and film thickness, i.e., the quantum interference effect. The oscillations become weaker in the thicker films due to the limited inelastic mean free path of NiO. Although it is hard to quantitatively determine the mean free path of NiO, our results suggest that the mean free path should be less than 14 ML, similar to that in MgO thin films.<sup>29</sup> It should be noted that the reflectivity spectra with the NiO thickness less than 10 ML in Fig. 2(c) exhibit discrete peaks at integer layers of the NiO thickness, indicating layer-by-layer growth mode of thin NiO films.<sup>39,40</sup> Those discrete peaks can be applied to calibrate the NiO thickness of the NiO films. Figure 3(a) and (b) show the energies of the reflectivity peaks as a function of NiO thickness for the energy ranges of 4–7.5 eV and 14–22 eV. Then, according to Eq. (1), the electron wave vector  $k(E)$  at a given energy  $E$  can be obtained from  $k(E) = \pi/\Lambda(E)$ , where  $\Lambda(E)$  is the oscillation period.

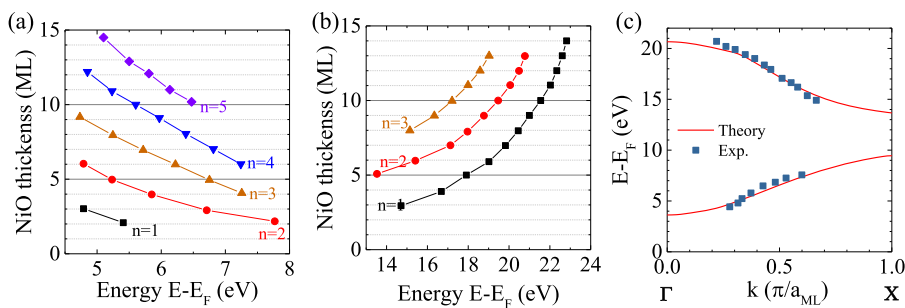


**FIG. 3.** The evolution of electron quantum interference maxima with fixed quantum number  $n$  as a function of film thickness and electron energy at (a) low energy range and (b) high energy range. (c) Experimental and calculated NiO unoccupied energy bands. The calculated energy bands are offset for best fit with the experimental data.

Therefore, the energy band dispersion can be derived experimentally from this quantum interference effect, as shown in Fig. 3(c). Note that the energy band dispersion of the NiO film can be determined entirely from the experimental data without the need of any models for the phase value.

To compare this measurement with theory, the band structure of NiO is calculated by density functional theory (DFT), using the Vienna *ab initio* simulation package (VASP 5.3.3).<sup>41</sup> Projector-augmented wave (PAW) potentials as parameterized by Perdew–Burke–Ernzerhof within the generalized gradient approximation (GGA) are used to account for electron exchange and correlation.<sup>42</sup> The projector augmentation wave potentials include sixteen valence electrons for Ni ( $3p^6 3d^8 4s^2$ ) and six for oxygen ( $2s^2 2p^4$ ). Considering the antiferromagnetic spin structure, we adopt the rhombohedral unit cell with  $Fm\bar{3}m$  space group (containing 2 chemical-formula units of NiO). Typical computational parameters for our calculations are a 520 eV plane-wave energy cut-off, a  $(8 \times 8 \times 8)$  Monkhorst–Pack  $k$ -point sampling mesh, and a 0.01 eV/Å force tolerance on each atom for structural relaxation calculations. To describe the electronic structure more accurately, we adopt the hybrid functional HSE06<sup>43</sup> to calculate the band structure. Our calculations reproduce the insulator nature of NiO with a band gap of about 4.36 eV, which is consistent with the experiment result of 4.3 eV.<sup>23</sup>

Figure 3(c) shows that the experimental data matches well with the theoretical calculation, supporting that the quantum interference effect of electron reflectivity is an effective method to determine the unoccupied band structure of the antiferromagnetic oxides. It is worth noting that there is a band gap between 7.5 eV and 14 eV, so no electron reflectivity oscillations can be observed in this energy range. The NiO film is expected to go through a phase transition from paramagnetic to AFM state with the transition thickness of 1 nm,<sup>44</sup> but the electron reflectivity spectra reveal no obvious transition at  $d_{\text{NiO}} \sim 5$  ML, so the measured NiO unoccupied band may be insensitive to the magnetic phase transition in the NiO film.

CoO has the same atomic structure as NiO, and can also be epitaxially grown on the Ag(001) surface. Thus, we have also studied the electron quantum interference effect in the CoO/Ag(001) system. Fig. 4 shows the electron reflectivity oscillation in the energy

range of 4–7.5 eV. However, the reflectivity oscillations from CoO films are weaker than that from NiO films. The quantum interference effect in CoO films disappears for thickness above 7 ML, and this may indicate that the electron in CoO film has shorter mean free path than in NiO film. On the other hand, our results also indicate that the surface morphology of CoO film is not as good as that of NiO film, since the discrete peaks of reflectivity at integer layers can only be observed for the CoO thickness less than 5 ML. The poorer surface smoothness can reduce the electron reflectivity and makes the oscillations weaker. The quantum interference effect is harder to be observed in the unoccupied band with the electron energy higher than 11 eV, and this is due to the short mean free path for higher electron energies. Since the quantum interference effect is only observed in very thin CoO films, it is difficult to use the phase accumulation model to derive the reliable CoO unoccupied energy band from the experimental data in Fig. 4.

## SUMMARY

We have studied the electron reflectivity from NiO and CoO thin films grown on Ag(001) using SPLEEM. Quantum interference induced oscillatory electron reflectivity as a function of film thickness and electron energy has been observed. The unoccupied band dispersion of NiO along the  $\Gamma$ –X direction is derived experimentally through the phase accumulation model, and agrees well with first principles calculations. Our work demonstrates that the quantum interference effect of electrons in AFM oxide thin films can be used to probe the unoccupied electronic structure above the Fermi surface, which can help to refine the understanding on the band structure of AFM oxides and is highly relevant to the development of novel AFM spintronic devices.

## ACKNOWLEDGMENTS

The work at Fudan University was supported by the National Key Basic Research Program of China (Grant No. 2015CB921401), National Key Research and Development Program of China (Grant No. 2016YFA0300703), National Natural Science Foundation of China (Grants No. 11974079, No. 11734006, No. 11825403), the Program of Shanghai Academic Research Leader (No. 17XD1400400), and Qing Nian Ba Jian Program. Work at the University of California, Davis was supported by the UC Office of the President Multi-campus Research Programs and Initiatives MRP-17-454963 and NSF DMR-1610060. Work at the Molecular Foundry was supported by the Office of Science, Office of Basic Energy Sciences, of the U.S. Department of Energy under Contract No. DE-AC02-05CH11231.

## REFERENCES

- <sup>1</sup>T. Jungwirth, X. Marti, P. Wadley, and J. Wunderlich, *Nat. Nanotechnol.* **11**, 231 (2016).
- <sup>2</sup>V. Baltz, A. Manchon, M. Tsoi, T. Moriyama, T. Ono, and Y. Tserkovnyak, *Rev. Mod. Phys.* **90**, 015005 (2018).
- <sup>3</sup>L. Baldatti, A. Ross, T. Niizeki, C. Schneider, R. Ramos, J. Cramer, O. Gomonay, M. Filianina, T. Savchenko, D. Heinze, A. Kleibert, E. Saitoh, J. Sinova, and M. Kläui, *Phys. Rev. B* **98**, 024422 (2018).
- <sup>4</sup>J. Fischer, O. Gomonay, R. Schlitz, K. Ganzhorn, N. Vlietstra, M. Althammer, H. Huebl, M. Opel, R. Gross, S. T. B. Goennenwein, and S. Geprags, *Phys. Rev. B* **97**, 014417 (2018).

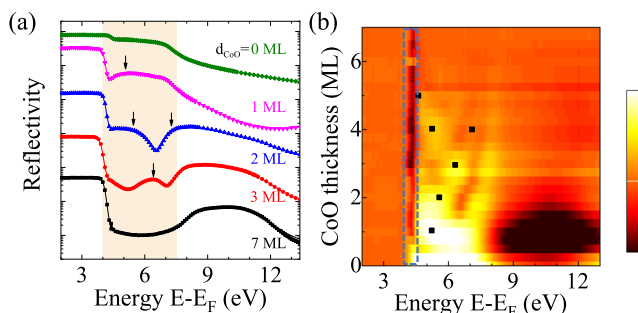


**FIG. 4.** (a) Electron reflectivity as a function of electron energy at different CoO thicknesses. Black arrows indicate quantum interference peaks in the reflectivity spectra. (b) Electron reflectivity versus thickness and the electron energy, normalized by the spectrum of 7ML CoO. The black squares indicate the reflectivity peaks with the quantization condition as described in Eq. (1). The blue rectangle indicates the area affected by the normalization process.



- <sup>5</sup>D. Hou, Z. Qiu, J. Barker, K. Sato, K. Yamamoto, S. Velez, J. M. Gomez-Perez, L. E. Hueso, F. Casanova, and E. Saitoh, *Phys. Rev. Lett.* **118**, 147202 (2017).
- <sup>6</sup>T. Shang, Q. F. Zhan, H. L. Yang, Z. H. Zuo, Y. L. Xie, L. P. Liu, S. L. Zhang, Y. Zhang, H. H. Li, B. M. Wang, Y. H. Wu, S. Zhang, and R.-W. Li, *Appl. Phys. Lett.* **109**, 032410 (2016).
- <sup>7</sup>W. Lin, K. Chen, S. Zhang, and C. L. Chien, *Phys. Rev. Lett.* **116**, 186601 (2016).
- <sup>8</sup>H. Wang, C. Du, P. C. Hammel, and F. Yang, *Phys. Rev. Lett.* **113**, 097202 (2014).
- <sup>9</sup>C. Hahn, G. de Loubens, V. V. Naletov, J. Ben Youssef, O. Klein, and M. Viret, *EPL* **108**, 57005 (2014).
- <sup>10</sup>T. Moriyama, S. Takei, M. Nagata, Y. Yoshimura, N. Matsuzaki, T. Terashima, Y. Tserkovnyak, and T. Ono, *Appl. Phys. Lett.* **106**, 162406 (2015).
- <sup>11</sup>C. Tzschaschel, K. Otani, R. Iida, T. Shimura, H. Ueda, S. Günther, M. Fiebig, and T. Satoh, *Phys. Rev. B* **95**, 174407 (2017).
- <sup>12</sup>S. Baierl, J. H. Mentink, M. Hohenleutner, L. Braun, T. M. Do, C. Lange, A. Sell, M. Fiebig, G. Woltersdorf, T. Kampfrath, and R. Huber, *Phys. Rev. Lett.* **117**, 197201 (2016).
- <sup>13</sup>T. Moriyama, K. Oda, T. Ohkochi, M. Kimata, and T. Ono, *Sci. Rep.* **8**, 14167 (2018).
- <sup>14</sup>X. Z. Chen, R. Zarzuela, J. Zhang, C. Song, X. F. Zhou, G. Y. Shi, F. Li, H. A. Zhou, W. J. Jiang, F. Pan, and Y. Tserkovnyak, *Phys. Rev. Lett.* **120**, 207204 (2018).
- <sup>15</sup>O. G. L. Baldtrati, A. Ross, M. Filianina, R. Lebrun, R. Ramos, C. Leveille, T. Forrest, F. Maccherozzi, E. Saitoh, J. Sinova, and M. Kläui, *arXiv:1810.11326* (2018).
- <sup>16</sup>W. L. Roth, *Phys. Rev.* **110**, 1333 (1958).
- <sup>17</sup>K. Terakura, A. R. Williams, T. Oguchi, and J. Kübler, *Phys. Rev. Lett.* **52**, 1830 (1984).
- <sup>18</sup>F. Tran and P. Blaha, *Phys. Rev. Lett.* **102**, 226401 (2009).
- <sup>19</sup>E. Engel and R. N. Schmid, *Phys. Rev. Lett.* **103**, 036404 (2009).
- <sup>20</sup>C.-Y. Kuo, T. Haupricht, J. Weinen, H. Wu, K.-D. Tsuei, M. W. Haverkort, A. Tanaka, and L. H. Tjeng, *Eur. Phys. J. Special Topics* **226**, 2445 (2017).
- <sup>21</sup>A. N. Mansour, *Surf. Sci. Spectra* **3**, 231 (1994).
- <sup>22</sup>A. P. Grosvenor, M. C. Biesinger, R. S. C. Smart, and N. S. McIntyre, *Surf. Sci.* **600**, 1771 (2006).
- <sup>23</sup>G. A. Sawatzky and J. W. Allen, *Phys. Rev. Lett.* **53**, 2339 (1984).
- <sup>24</sup>Z.-X. Shen, R. S. List, D. S. Dessau, B. O. Wells, O. Jepsen, A. J. Arko, R. Bartlett, C. K. Shih, F. Parmigiani, J. C. Huang, and P. A. P. Lindberg, *Phys. B: Condens. Matter* **44**, 3604 (1991).
- <sup>25</sup>C.-M. Cheng, C.-C. Wang, H.-T. Jeng, C. S. Hsue, B. Y. Hsu, D.-J. Huang, and K.-D. Tsuei, *Phys. B: Condens. Matter* **403**, 1539 (2008).
- <sup>26</sup>R. Zdyb and E. Bauer, *Phys. Rev. Lett.* **88**, 166403 (2002).
- <sup>27</sup>J. S. Park, A. Quesada, Y. Meng, J. Li, E. Jin, H. Son, A. Tan, J. Wu, C. Hwang, H. W. Zhao, A. K. Schmid, and Z. Q. Qiu, *Phys. Rev. B* **83**, 113405 (2011).
- <sup>28</sup>J. Graf, C. Jozwiak, A. K. Schmid, Z. Hussain, and A. Lanzara, *Phys. Rev. B* **71**, 144429 (2005).
- <sup>29</sup>Y. Z. Wu, A. K. Schmid, M. S. Altman, X. F. Jin, and Z. Q. Qiu, *Phys. Rev. Lett.* **94**, 027201 (2005).
- <sup>30</sup>T. Ohta, F. El Gabaly, A. Bostwick, J. L. McChesney, K. V. Emtsev, A. K. Schmid, T. Seyller, K. Horn, and E. Rotenberg, *New J. Phys.* **10**, 023034 (2008).
- <sup>31</sup>Y. Z. Wu, A. K. Schmid, and Z. Q. Qiu, *Phys. Rev. Lett.* **97**, 217205 (2006).
- <sup>32</sup>A. M. Shikin, D. V. Vyalikh, G. V. Prudnikova, and V. K. Adamchuk, *Surf. Sci.* **487**, 135 (2001).
- <sup>33</sup>A. Danese and R. A. Bartynski, *Phys. Rev. B* **65**, 174419 (2002).
- <sup>34</sup>N. Rougemaille and A. K. Schmid, *Eur. Phys. J. Appl. Phys.* **50**, 20101 (2010).
- <sup>35</sup>H. Yang, G. Chen, A. A. C. Cotta, A. T. N'Diaye, S. A. Nikolaev, E. A. Soares, W. A. A. Macedo, K. Liu, A. K. Schmid, A. Fert, and M. Chshiev, *Nat. Mater.* **17**, 605 (2018).
- <sup>36</sup>Y. Z. Wu, Z. Q. Qiu, Y. Zhao, A. T. Young, E. Arenholz, and B. Sinkovic, *Phys. Rev. B* **74**, 212402 (2006).
- <sup>37</sup>P. Sheng, F. Bonell, S. Miwa, T. Nakamura, Y. Shiota, S. Murakami, D. D. Lam, S. Yoshida, and Y. Suzuki, *Appl. Phys. Lett.* **102**, 032406 (2013).
- <sup>38</sup>S. Starfelt, H. M. Zhang, and L. S. O. Johansson, *Phys. Rev. B* **97**, 195430 (2018).
- <sup>39</sup>K. L. Kostov, S. Polzin, F. O. Schumann, and W. Widdra, *Surf. Sci.* **643**, 23 (2016).
- <sup>40</sup>C. Giovanardi, A. di Bona, S. Altieri, P. Luches, M. Liberati, F. Rossi, and S. Valeri, *Thin Solid Films* **428**, 195 (2003).
- <sup>41</sup>G. Kresse and J. Furthmüller, *Phys. Rev. B* **54**, 11169 (1996).
- <sup>42</sup>J. P. Perdew, K. Burke, and M. Ernzerhof, *Phys. Rev. Lett.* **77**, 3865 (1996).
- <sup>43</sup>A. V. Krukau, O. A. Vydrov, A. F. Izmaylov, and G. E. Scuseria, *J. Chem. Phys.* **125**, 224106 (2006).
- <sup>44</sup>D. Alders, L. H. Tjeng, F. C. Voogt, T. Hibma, G. A. Sawatzky, C. T. Chen, J. Vogel, M. Sacchi, and S. Iacubucci, *Phys. Rev. B* **57**, 11623 (1998).